

# Dynamic Behavior of Thin Graphite/Epoxy FRP Simply Supported Beam Under Thermal Load Using 3-D Finite Element Modeling

Fadi Alfaqs

Department of Mechanical Engineering, Faculty of Engineering Technology, Al-Balqa Applied University, Jordan

Received November 18 2020

Accepted June 23 2021

## Abstract

Composite laminated structures have attracted much attention in recent years due to their wide range of mechanical properties and applications. However, this study presents an investigation of temperature impact as well as fiber orientation effect on mid-plane transverse deflection and interlaminar shear stress as the latter plays a crucial role in the layers' delamination in eight-layer laminated simply supported Graphite/Epoxy FRP composite beam. The beam considered is subjected to dynamic force of magnitude 1000 N concentrated in the middle as frequency varies 5-50 Hz using 3-D finite element modeling where different fiber orientations ( $[0^\circ]_8$ ,  $[0^\circ/15^\circ]_s$ ,  $[0^\circ/30^\circ]_s$ ,  $[0^\circ/45^\circ]_s$ ,  $[0^\circ/60^\circ]_s$ ,  $[0^\circ/75^\circ]_s$ , and  $[0^\circ/90^\circ]_s$ ) are considered for temperature 22, 40, and 60°C. Furthermore, modal analyses are carried out for all fiber orientations and temperatures considered. Results obtained via this study show that natural frequencies' values drop narrowly when the temperature applied on the structure rises. Moreover, dynamic mid-plane transverse and interfacial shear stress increases when increasing temperature. It should be said that comparing fiber orientations considered for every single temperature across the frequency range, fiber orientation scheme  $[0^\circ]_8$  recorded minimum transverse deflection and maximum shear stress.

© 2021 Jordan Journal of Mechanical and Industrial Engineering. All rights reserved

**Keywords:** Laminated Beam; Dynamic; Modal, interlaminar Shear stress; Finite element;

## 1. Introduction

Failure of composite structures due to layers delamination is widely studied in literature where interlaminar shear stress between laminates is considered one of the main reasons of layers debonding. Normal stress effect on interlaminar shear stress of composite structures was studied where improved model of multiple notch experiments was used [1]. Moreover, method of characteristic curve was investigated in specimens containing double notches. Results obtained were compared to several failure criteria where excellent agreement was found with NU criterion. However, a review of different laminates' simulation of composite structures was presented [2]. This work studied the impact of different loading conditions on the delamination process and compared to failure models. Also, experimental results concerning toughness and impact resistance under different loading conditions were discussed.

Analytical investigation of fiber reinforced polymer (FRP) used in concrete beams subjected to impact loading was carried out to improve the beams considered [3]. However, several loading types and structures' geometry were studied using finite element (FE) package ABAQUS where models were developed using different configurations. Numerical results obtained via the FE software showed reliability concerning performance prediction of the beams considered. On the other hand, the

effect of SiC particles filled with different types of laminates was studied on interlaminar shear strength [4]. Different percentages of SiC were investigated experimentally where fractured areas were observed by electron scanner and optical microscopy as well. It is found that shear strength of laminates with SiC particles is significantly improved compared to the same structures containing no SiC particles.

Visco-plasticity was considered in failure analysis of FRP laminated composite structures when undergoing high strain rates using constitutive model [5]. Results obtained that the model considered shows the ability to predict strength of laminates in the composite structures when compared to experimental results. However, a review of dynamic behavior of FRP composite structures were investigated for several loading speeds [6]. Furthermore, effect of different strain rates of tension and compression were studied in order to observe laminates' failure for different composites.

Finite element analysis was performed to investigate the damage of FRP composites [7]. In addition, experiments were conducted to analyze the damage induced by drilling process where results were compared to finite element results obtained. On the other hand, FRP laminated composites subjected to two low velocity cylindrical impacts were investigated using finite element modeling to assess the delamination of mechanical structures' plies [8]. Also, delamination criterion was used to specify the location of the delamination. It is found that interfacial

\* Corresponding author e-mail: faalfaq@bau.edu.jo.

delamination is significantly affected by the time between the two impacts applied.

Dynamic behavior FRP walls containing debonded regions was studied and analyzed where finite element models were developed to observe the nonlinear dynamic behavior [9]. In addition, von Karman criteria for different shear loads was used to model the geometry resulted from debonded regions. Results showed crucial effect of the regions considered on the dynamic behavior of the analyses. However, interlaminar normal and shear stresses were evaluated for different orientation schemes of FRP mechanical composite structures [10]. It is found laminates with fiber angles of 45° achieve maximum interfacial stresses.

Different parameters such as stacking schemes and boundary conditions were studied to evaluate the delamination process in carbon FRP laminated composite plate using FE package ANSYS [11]. Furthermore, Analytical formula was developed using Rayleigh-Ritz method and results were computed using MATLAB. It is found that fixed boundary conditions resulted in larger delamination size than simply supported conditions. Moreover, excellent agreement was observed between analytical and FE results.

Impact of thermal loading on free edge in mechanical structures were studied through developing new 2-D plane strain equations [12]. Moreover, Finite element analysis was used to implement the criteria considered to verify the results obtained. Results obtained in this work showed that interfacial stresses are well predicted when thermal load was applied locate the delaminated regions in the mechanical structure.

Effect of temperature on interfacial shear stress existing between laminates was investigated in carbon FRP composite structures [13]. Such an impact was observed using double notch shear experimental test where results were compared to a developed FE model. It is found that failure occurs due to epoxy resin softening. However, many static and dynamic experiments were carried out For bi-directional glass FRP materials to observe and analyze failure process [14]. Experimental Results obtained shows modulus of elasticity change in all three directions for different dynamic strain rates.

Dynamic and static analysis of FRP materials were studied for several environmental conditions using different types of loads including temperature [15]. In this work, failure was observed through the delaminated regions which lead eventually to material damage. It is found that environmental conditions such as temperature plays a significant role in failure process. Furthermore, thermoelastic study was conducted to investigate delamination properties of FRP composite structures where FE models were performed [16]. This analysis was concerned about the failure of laminates caused by thermal and structural conditions. It is found that stress induced thermally play a crucial role in facial delamination in mechanical composite structures.

Experimental shear tests were carried out in laminated composites where interfacial shear strength was measured through MSBS tests [17]. Moreover, FE model was developed to evaluate the results which showed clearly that a correction is needed for the equation of shear stress theory. However, structural and thermal interlaminar stresses are investigated for laminated composite shells using FE analysis [18]. The study used different fiber orientation schemes to monitor the stresses considered. Where critical interfaces were located throughout the structure.

Analysis of shear stress behavior was performed for epoxy resin- FRP composites as well as E-glass FRP laminated structures [19]. The study examined different resins and fibers. It is found that the model developed predicted the interfacial shear strength accurately. On the other hand, interlaminar shear stresses induced by harmonic and transient loads are examined for different viscoelastic laminated structures with different loading conditions [20,21]. FE model was performed to study these interfacial stresses where it is found that shear stress plays a crucial load in delamination process specially at natural frequencies. Furthermore, dynamic interlaminar shear stresses at midplane of composite simply supported thin plate were studied in different stacking fiber orientation order at several temperatures using FE package ANSYS [22]. Results revealed that increasing temperature leads to shear stress increase for all orientations considered.

FE vibration analysis of composite plates for different conditions was reviewed and simulated using ANSYS and ABAQUS softwares where it is found that natural frequencies drops when increasing the size of delamination [23,24]. However, Analytical work of composite beams was performed to study dynamic response of such beams for different conditions and materials [25,26].

In this study, FE modeling of thin simply Graphite/Epoxy laminated simply supported beam is carried out using FE package ANSYS19 in order to perform both modal and dynamic analyses of mid-plane deflections and interlaminar shear stresses under the effect of different temperature values 22, 40, and 60°C for different fiber orientation schemes ([0°]<sub>s</sub>, [0°/15°]<sub>s</sub>, [0°/30°]<sub>s</sub>, [0°/45°]<sub>s</sub>, [0°/60°]<sub>s</sub>, [0°/75°]<sub>s</sub>, and [0°/90°]<sub>s</sub>).

## 2. Material Properties

Physical Properties of the materials used in modeling thin simply supported beam considered consisting of eight bonded perfectly layers are listed in table I. It should be mentioned that since the material is orthotropic, physical properties differ from direction to another.

**Table1.** Physical properties of Graphite/Epoxy FRP material used (Gu, et al.)[27]

	Direction 1	Direction 2	Direction 3
Density (Kg/m <sup>3</sup> )	1610	-	-
Modulus of Elasticity (GPa)	144.23	9.65	9.65
Shear Modulus (GPa)	G <sub>12</sub> = 3.45	G <sub>13</sub> = 4.14	G <sub>23</sub> = 4.14
Poisson's ratio	ν <sub>12</sub> = 0.3	ν <sub>13</sub> = 0.3	ν <sub>23</sub> = 0.3
Thermal expansion (°C <sup>-1</sup> )	1.1 E-6	25.2 E-6	25.2 E-6
Thermal Conductivity (Wm <sup>-1</sup> K <sup>-1</sup> )	48.44	0.8	0.8

## 3. Finite Element and Mathematical Modeling

3-D Finite element modeling of Graphite/Epoxy FRP simply supported laminated beam is performed using ANSYS19 where solid186 elements are being utilized to

mesh the beam considered as depicted in Fig 1. It should be said that these elements contain 20 nodes each and are capable of both structural and thermal FE analyses. Moreover, accuracy of results is improved compared to solid185 elements since the latter consists of 8 nodes. The length of the beam  $L$  is 1000mm as shown in Fig. 2 while the width is 50mm. However, each laminated layer thickness is modeled as 6.25mm. The force  $F$  which represents a dynamic force with amplitude 1000N is concentrated at the middle of the simply supported beam considered.

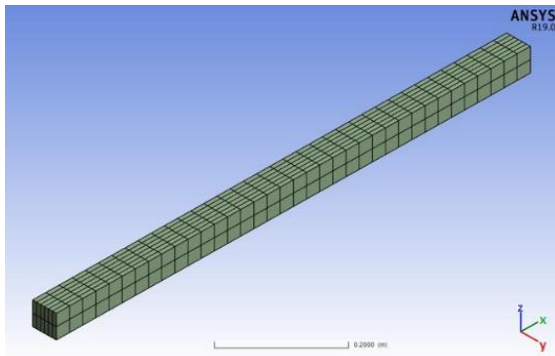


Figure1. Finite element model of simply supported beam

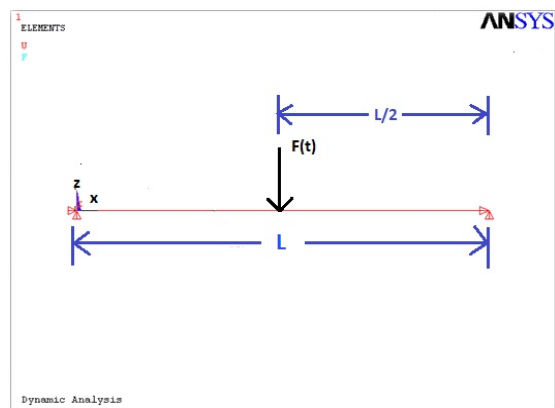


Figure2.Design Scheme for the simply supported composite beam

FE model is verified using the results obtained for free edge laminated plate [28] as shown in Fig. 3. Results obtained in current model present excellent agreement with the corresponding literature results where the free edge laminated FRP plate contains 8 layers of stacking sequence  $[0/90]_s$ . It should be said that the mechanical properties are stated in Table I .

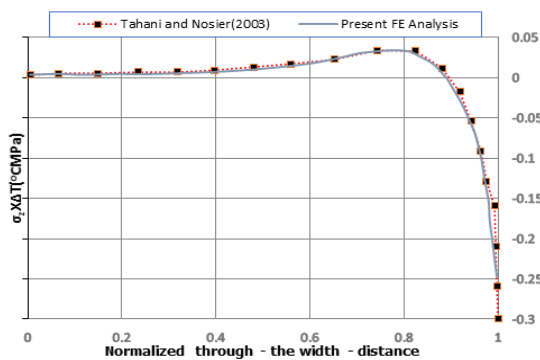


Figure3.Interfacial normal stress of free edge Graphite/Epoxy plate of an orientation scheme  $[0/90]_s$  for a temperature change  $1^\circ\text{C}$  (Tahani et al[22])

Fig. 4 represents the stacking sequence for a composite laminated structure. As in current case study, there are eight laminated layers in which 4 layers above midplane and same number of layers under the mid plane as well.

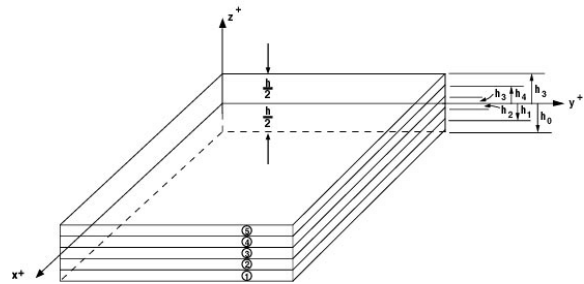


Figure4.Stacking Sequence of laminated structure

On the other hand, it should be mentioned that displacement relations according to the shear deformation theory in laminated beam are expressed as

$$\begin{aligned}
 U(x, y, z) &= u_0(x, y) - z \frac{\partial w}{\partial x}(x, y) + f(z)\Phi(x, y) \\
 V(x, y, z) &= v_0(x, y) - z \frac{\partial w}{\partial y}(x, y) + f(z)\psi(x, y) \\
 W(x, y) &= w(x, y)
 \end{aligned} \quad (1)$$

Where  $U$ ,  $V$ , and  $W$  are mid-plane displacements in  $x, y$ , and  $z$  directions respectively.  $\Phi$  and  $\psi$  are shear rotations.  $f(z)$  is distribution function.

Assuming small displacements, strain-displacement relations become

$$\begin{aligned}
 \epsilon_x &= \frac{\partial U}{\partial x}, \epsilon_y = \frac{\partial V}{\partial y}, \epsilon_z = \frac{\partial W}{\partial z} \\
 \gamma_{xy} &= \frac{\partial U}{\partial y} + \frac{\partial V}{\partial x}, \gamma_{xz} = \frac{\partial U}{\partial z} + \frac{\partial W}{\partial x} \\
 \gamma_{yz} &= \frac{\partial V}{\partial z} + \frac{\partial W}{\partial y}
 \end{aligned} \quad (2)$$

Hence equation (1) becomes

$$\begin{aligned}
 \epsilon_x &= \frac{\partial u_0}{\partial x} - z \frac{\partial^2 w}{\partial x^2} + f(z) \frac{\partial \Phi}{\partial x} \\
 \epsilon_y &= \frac{\partial v_0}{\partial y} - z \frac{\partial^2 w}{\partial y^2} + f(z) \frac{\partial \Phi}{\partial y} \\
 \epsilon_z &= 0 \\
 \gamma_{xy} &= \frac{\partial u_0}{\partial y} + \frac{\partial v_0}{\partial x} - 2z \frac{\partial^2 w}{\partial x \partial y} + f(z) \left( \frac{\partial \Phi}{\partial y} + \frac{\partial \psi}{\partial x} \right)
 \end{aligned} \quad (3)$$

$$\begin{aligned}
 \gamma_{yz} &= \frac{\partial f(z)}{\partial y} \Phi \\
 \gamma_{xz} &= \frac{\partial f(z)}{\partial z} \psi
 \end{aligned}$$

However, considering thermal effect and shear deformations, stress-strain relations become in the  $k$ th layer

$$\begin{Bmatrix} \sigma_x \\ \sigma_y \\ \tau_{xy} \\ \tau_{yz} \\ \tau_{xz} \end{Bmatrix}^k = \begin{bmatrix} Q_{11} & Q_{12} & 0 & 0 & 0 \\ Q_{21} & Q_{22} & 0 & 0 & 0 \\ 0 & 0 & Q_{66} & 0 & 0 \\ 0 & 0 & 0 & Q_{44} & 0 \\ 0 & 0 & 0 & 0 & Q_{55} \end{bmatrix} \begin{Bmatrix} \epsilon_x - \alpha_x T \\ \epsilon_y - \alpha_y T \\ \gamma_{xy} \\ \gamma_{yz} \\ \gamma_{xz} \end{Bmatrix}^k \quad (4)$$

Where  $\alpha_x$  and  $\alpha_y$  are thermal expansion coefficients in x any directions respectively. T is thermal load  $Q_{ij}$  is transformed elastic coefficients

$$Q_{11} = \frac{E_1}{1 - \nu_{12}\nu_{21}}, Q_{12} = \frac{\nu_{21}E_2}{1 - \nu_{12}\nu_{21}},$$

$$Q_{22} = \frac{E_2}{1 - \nu_{12}\nu_{21}}$$

$$Q_{66} = G_{12}, Q_{55} = G_{13}, Q_{44} = G_{23}$$

Where  $E_1$  and  $E_2$  are material modulus of elasticity in principle directions 1 and 2 respectively.  $\nu_{12}\nu_{21}$  are Poisson's ratios and  $G_{12}, G_{13},$  and  $G_{23}$  are material modulus of rigidity.

**4. Results and Discussion**

Natural frequencies of Graphite/Epoxy composite simply supported laminated beam are obtained by performing modal analysis using 3-D finite element modeling in Ansys19 for different fiber orientation angles ( $[0^\circ]_s, [0^\circ/15^\circ]_s, [0^\circ/30^\circ]_s, [0^\circ/45^\circ]_s, [0^\circ/60^\circ]_s, [0^\circ/75^\circ]_s,$  and  $[0^\circ/90^\circ]_s$ ) at temperatures 22, 40, and 60°C as shown in tables 2, 3, and 4. Table. 2 presents the first six natural frequencies of the composite simply supported beam at 22°C for all fiber orientation schemes considered. It should be observed that should temperature increases natural frequencies decreases slightly. Furthermore, largest natural frequency 258.56Hz is obtained for fiber orientation scheme  $[0^\circ]_s$ .

It is clearly observed that largest fundamental natural frequency is recorded at a fiber orientation scheme  $[0^\circ]_s$ . However, it should be said that lowest fundamental natural frequencies are obtained for orientation schemes  $[0^\circ/60^\circ]_s, [0^\circ/75^\circ]_s,$  and  $[0^\circ/90^\circ]_s$  for all temperatures considered.

The first six natural frequencies are listed for all fiber orientation schemes considered for 22, 40, and 60°C as listed in table. 3 and table. 4, where it is clearly observed that highest natural frequencies are recorded at fiber

orientation scheme  $[0^\circ]_s$  as 258.4 and 258.23 Hz at temperatures 40 and 60°C respectively.

Dynamic analysis for Graphite/Epoxy FRP simply supported beam is carried out using finite element modeling for fiber orientation schemes  $[0^\circ]_s, [0^\circ/15^\circ]_s, [0^\circ/30^\circ]_s, [0^\circ/45^\circ]_s, [0^\circ/60^\circ]_s, [0^\circ/75^\circ]_s,$  and  $[0^\circ/90^\circ]_s$  at temperatures 22, 40, and 60°C where the magnitude of force is 1000N concentrated at the middle of the beam considered. It should be mentioned that current analysis is performed for frequency range 5 – 50Hz to observe closely the effect of temperature on transverse deflection and interfacial shear stress of mid-plane at L/2. Fig. 5. shows the relation of transverse deflection of fiber angle  $[0^\circ]_s$  for the three different temperatures considered. Generally, transverse deflection of mid-plane increases when temperature increases across driving frequency variation 5-50Hz. However, maximum transverse deflection is recorded 82.7mm at frequency 285Hz and temperature 22°C when modeling the simply supported beam for frequency variation 0-300 Hz. This result indicates that while higher temperature application induces higher midplane deflection, maximum deflection is obtained at room temperature (22°C) when the driving frequency matches the second natural frequency.

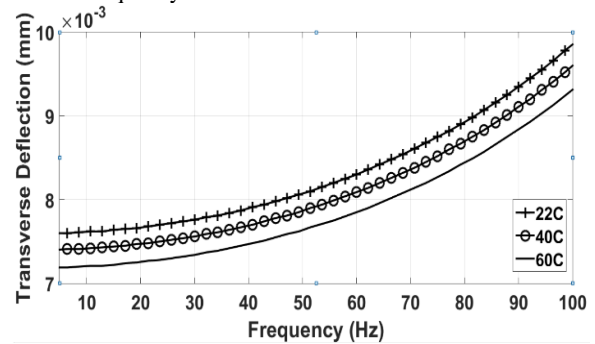


**Figure5.** Relation between mid-plane transverse deflection and driving frequency for Graphite/Epoxy laminated simply supported beam for  $[0^\circ]_s$  at temperatures 22, 40, and 60°C

**TABLE 2.** Natural frequencies of composite laminated simply supported FRP beam for different orientation at temperature 22 °C

Mode	$[0^\circ]_s$	$[0^\circ/15^\circ]_s$	$[0^\circ/30^\circ]_s$	$[0^\circ/45^\circ]_s$	$[0^\circ/60^\circ]_s$	$[0^\circ/75^\circ]_s$	$[0^\circ/90^\circ]_s$
1	258.56	238.53	220.35	211.5	208.99	208.81	209.02
2	285.37	247.15	227.78	223.25	220.15	217.82	216.86
3	667.38	606.15	563.65	548.53	543.52	542.86	543.25
4	718.7	710.86	680.11	663.2	648.06	635.12	629.62
5	759.47	735.81	738.88	721.65	693.83	667.47	656.12
6	1332.3	1309.2	1223.6	1189.2	1176.5	1173.4	1173.5

**TABLE 3.** Natural frequencies of composite laminated simply supported FRP beam for different orientation at temperature 40 ° C

Mode	$[0^\circ]_s$	$[0^\circ/15^\circ]_s$	$[0^\circ/30^\circ]_s$	$[0^\circ/45^\circ]_s$	$[0^\circ/60^\circ]_s$	$[0^\circ/75^\circ]_s$	$[0^\circ/90^\circ]_s$
1	258.4	238.39	220.22	211.36	208.82	208.61	208.8
2	285.21	247	227.66	223.12	220	217.64	216.67
3	667.31	605.93	563.43	548.3	543.27	542.57	542.94
4	718.46	710.73	679.99	663.06	647.9	634.92	629.4
5	759.33	735.75	738.85	721.61	693.77	667.39	656.04
6	1332.1	1308.9	1223.4	1189	1176.3	1173.1	1173.2

**TABLE 4.** natural frequencies of composite laminated simply supported FRP beam for different orientation at temperature 60 ° C

Mode	$[0^\circ]_s$	$[0^\circ/15^\circ]_s$	$[0^\circ/30^\circ]_s$	$[0^\circ/45^\circ]_s$	$[0^\circ/60^\circ]_s$	$[0^\circ/75^\circ]_s$	$[0^\circ/90^\circ]_s$
1	258.23	238.24	220.06	211.2	208.63	208.39	208.57
2	285.04	246.84	227.53	222.98	219.83	217.44	216.45
3	667.23	605.69	563.19	548.05	542.99	542.25	542.59
4	718.19	710.57	679.86	662.91	647.71	634.69	629.16
5	759.17	735.68	738.81	721.56	693.7	667.31	655.96
6	1331.9	1308.7	1223.1	1188.8	1176	1172.8	1172.8

Dynamic mid plane deflection results of fiber orientation scheme  $[0^\circ/15^\circ]_s$  at different temperatures are shown in Fig. 6 for frequency range 5 – 50Hz. It should be said that close values of deflection are obtained at temperatures 40 and 60°C and lower deflections are recorded when modeling at 22°C. However, comparing current scheme results with those of  $[0^\circ]_s$  case, it can be concluded that mid-plane deflections of  $[0^\circ/15^\circ]_s$  are much higher than the latter case which comes as a result of that the fibers angle in each laminate is longitudinal which adds strength to the mechanical structure. Furthermore, it should be noted that maximum mid-plane transverse deflection is 66.2mm at the second natural frequency when the temperature is set to 60°C.

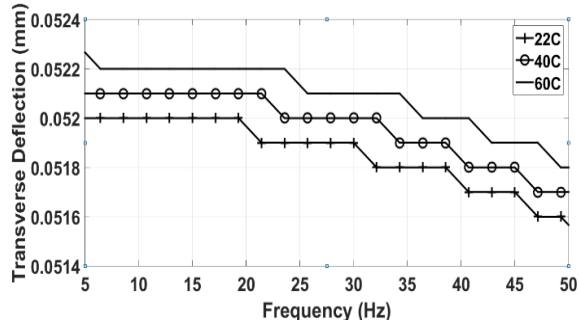


**Figure 6.** Relation between mid-plane transverse deflection and driving frequency for Graphite/Epoxy laminated simply supported beam for  $[0^\circ/15^\circ]_s$  at temperatures 22, 40, and 60°C

Moreover, effect of temperature on laminated Graphite/Epoxy simply supported beam with fiber orientation scheme  $[0^\circ/30^\circ]_s$  is investigated for frequency range 5 -50Hz and temperature variation 22, 40, and 60°C as shown in Fig. 7. It is clearly seen that should the temperature increases, harmonic deflection increases as well for driving frequency varies from 5-50Hz. It should be mentioned that maximum deflection is recorded 3.13mm at mid-plane at a frequency 220.7Hz for a temperature 22°C which represents a fundamental frequency.

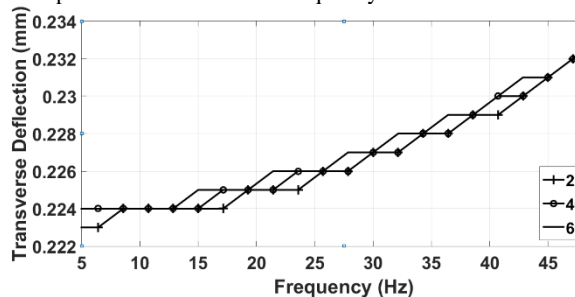


**Figure7.** Relation between mid-plane transverse deflection and driving frequency for Graphite/Epoxy laminated simply supported beam for  $[0^\circ/30^\circ]_s$  at temperatures 22, 40, and 60°C

However, Fig. 8 to Fig. 11 present the relation between midplane transverse deflection of the laminated Graphite/Epoxy simply supported beam for driving frequency variation 5 - 50Hz at different temperatures for fiber orientation schemes  $[0^\circ/45^\circ]_s$ ,  $[0^\circ/60^\circ]_s$ ,  $[0^\circ/75^\circ]_s$ , and  $[0^\circ/90^\circ]_s$  respectively. In general, same trend is observed as in previous schemes for most of the frequency range considered where it is found that increasing temperature will increase the transverse deflection induced by the

harmonic force. However, it is clearly observed in all figures considered that midplane deflection at temperatures 40 and 60°C where close results are obtained for some respectable frequency ranges. As for  $[0^\circ/45^\circ]_s$  and  $[0^\circ/60^\circ]_s$  cases, the frequency range 26 – 39Hz resulted in close mid-plane deflections. On the other hand, and for both orientation schemes mentioned, maximum transverse deflections are found to be 49.1 and 45.6mm respectively at the fundamental frequency and for temperature 22°C.

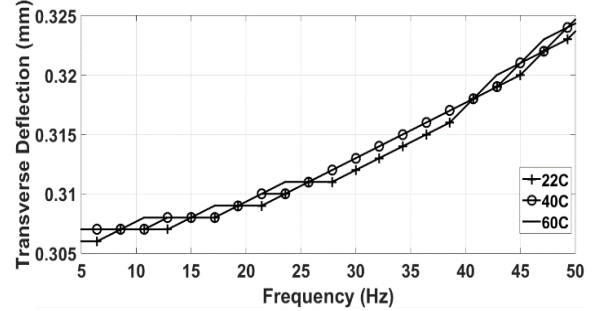


**Figure8.** Relation between mid-plane transverse deflection and driving frequency for Graphite/Epoxy laminated simply supported beam for  $[0^\circ/45^\circ]_s$  at temperatures 22, 40, and 60°C

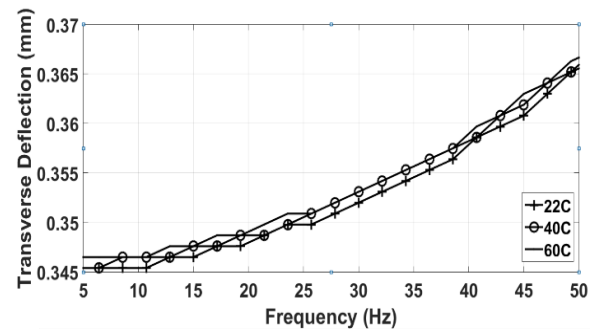


**Figure9.** Relation between mid-plane transverse deflection and driving frequency for Graphite/Epoxy laminated simply supported beam for  $[0^\circ/60^\circ]_s$  at temperatures 22, 40, and 60°C

In the same context, fiber orientation schemes  $[0^\circ/75^\circ]_s$  and  $[0^\circ/90^\circ]_s$  follow the same trend concerning the mid-plane deflection behavior of simply supported beam considered in current study where higher values are obtained for higher temperatures values across driving frequency 5 – 50 Hz. It is noted that maximum values of deflections for the schemes considered are 60.3 and 45.2mm induced at the fundamental frequency when temperature is 60°C.

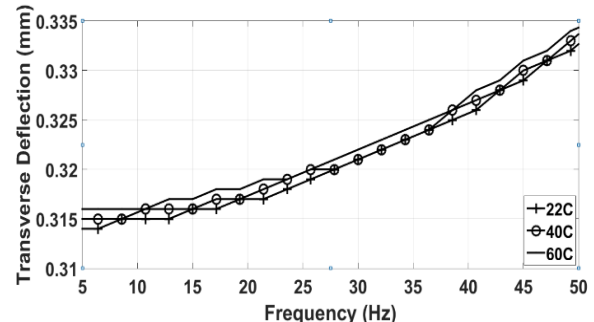


**Figure10.** Relation between mid-plane transverse deflection and driving frequency for Graphite/Epoxy laminated simply supported beam for  $[0^\circ/75^\circ]_s$  at temperatures 22, 40, and 60°C

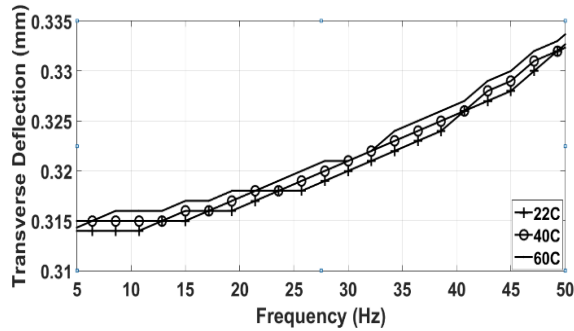


**Figure11.** Relation between mid-plane transverse deflection and driving frequency for Graphite/Epoxy laminated simply supported beam for  $[0^{\circ}/90^{\circ}]_s$  at temperatures 22, 40, and 60°C

Similarly, Harmonic analyses for eight-layer laminated Graphite/Epoxy simply supported beam is carried out for fiber orientation schemes  $[0^{\circ}]_s$ ,  $[0^{\circ}/15^{\circ}]_s$ ,  $[0^{\circ}/30^{\circ}]_s$ ,  $[0^{\circ}/45^{\circ}]_s$ ,  $[0^{\circ}/60^{\circ}]_s$ ,  $[0^{\circ}/75^{\circ}]_s$ , and  $[0^{\circ}/90^{\circ}]_s$  and temperature variation (22, 40, and 60°C) at frequency range (5 - 50Hz) as depicted in Fig. 12 to Fig. 18 respectively. It should be said that shear stresses are induced due to dynamic force concentrated in the middle of the beam (at  $L/2$ ). Fig. 12 investigates the effect of temperature on interfacial shear stress at mid plane for the orientation scheme  $[0^{\circ}]_s$  and frequency range considered. It is clearly observed that for most of the frequency range, dynamic interfacial shear stress at the midplane obtains higher values when temperature increases where maximum shear stress value 81.2 MPa is recorded at the fundamental frequency for temperature 60°C. This trend is also observed in Fig. 13, that is should the temperature increases, mid-plane shear stress of the beam considered rises for the orientation scheme  $[0^{\circ}/30^{\circ}]_s$ . Maximum magnitude of the interfacial shear stress at mid-plane is found to be 43.2MPa for temperature 60°C.

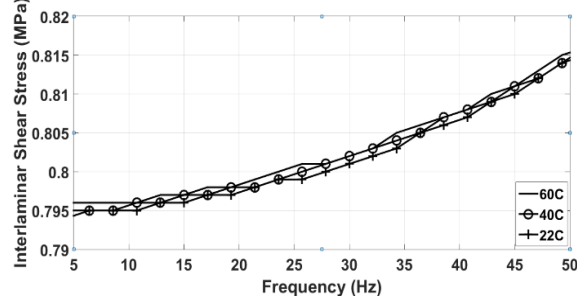


**Figure12.** Relation between mid-plane interfacial shear stress and driving frequency for Graphite/Epoxy laminated simply supported beam for  $[0^{\circ}]_s$  at temperatures 22, 40, and 60°C

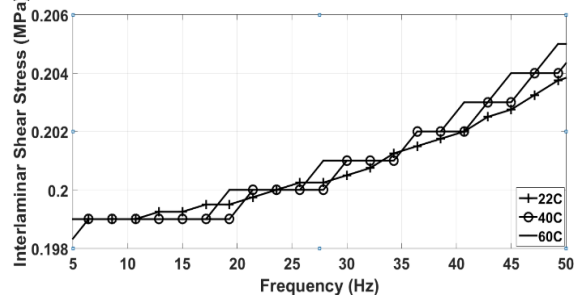


**Figure13.** Relation between mid-plane interfacial shear stress and driving frequency for Graphite/Epoxy laminated simply supported beam for  $[0^{\circ}/15^{\circ}]_s$  at temperatures 22, 40, and 60°C

However, the results of interlaminar shear stress obtained for frequency range 21 – 46Hz are nearly similar for temperatures 50 and 60°C for stacking sequence  $[0^{\circ}/30^{\circ}]_s$  as shown in Fig. 14. where Lowest values of stress are recorded for room temperature. It should be mentioned that maximum interfacial shear stress is recorded 0.017 MPa at the first natural frequency for temperature 22°C. Moreover, it can be clearly seen that there are constant values of shear stress at large portions of frequency for all temperatures considered.

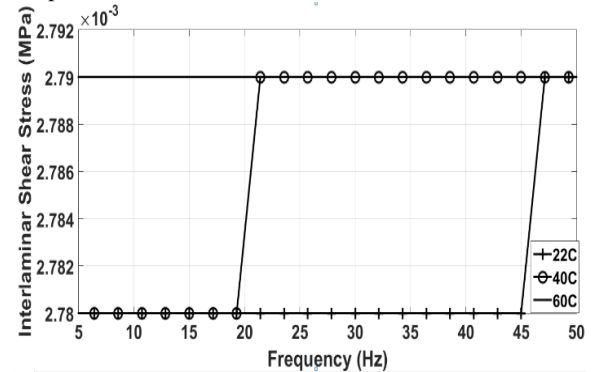


**Figure14.** Relation between mid-plane interfacial shear stress and driving frequency for Graphite/Epoxy laminated simply supported beam for  $[0^{\circ}/30^{\circ}]_s$  at temperatures 22, 40, and 60°C

Fig. 15 to Fig. 18 illustrate the impact of temperature on interlaminar shear stress at the mid-plane for the composite simply supported beam considered concerning orientation schemes  $[0^{\circ}/45^{\circ}]_s$ ,  $[0^{\circ}/60^{\circ}]_s$ ,  $[0^{\circ}/75^{\circ}]_s$ , and  $[0^{\circ}/90^{\circ}]_s$  respectively . It is clearly concluded that for all the cases considered increasing temperature leads to narrow interfacial shear stress increase at the mid plane. Also, it should be noted that a maximum shear stress of 17.8MPa for the fiber orientation scheme  $[0^{\circ}/45^{\circ}]_s$  is recorded at frequency 212.1HZ which represents a fundamental frequency for the scheme and temperature considered. In the same context, Maximum shear stress for orientations schemes  $[0^{\circ}/60^{\circ}]_s$ ,  $[0^{\circ}/75^{\circ}]_s$ , and  $[0^{\circ}/90^{\circ}]_s$  are found to be 8.27, 4.69, and 3.86Mpa respectively at the fundamental frequency computed in modal analyses at 60°C. Moreover, the nonlinear behavior observed in the shear stress response of the  $[0^{\circ}/90^{\circ}]_s$  case recorded very close results although same effect of temperature remains identical for rest of case considered.

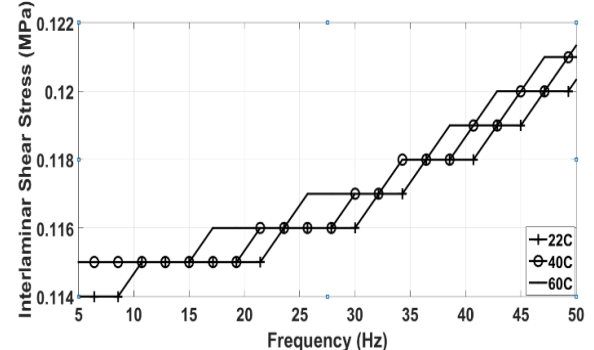


**Figure15.** Relation between mid-plane interfacial shear stress and driving frequency for Graphite/Epoxy laminated simply supported beam for  $[0^{\circ}/45^{\circ}]_s$  at temperatures 22, 40, and 60°C

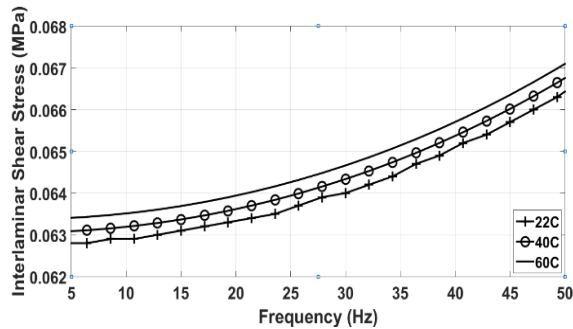


**Figure 16.** Relation between mid-plane interfacial shear stress and driving frequency for Graphite/Epoxy laminated simply supported beam for  $[0^\circ/60^\circ]_s$  at temperatures 22, 40, and  $60^\circ\text{C}$

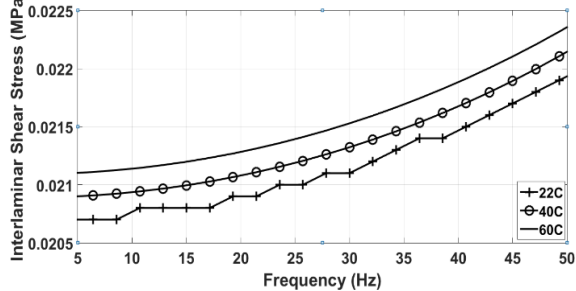


**Figure 17.** Relation between mid-plane interfacial shear stress and driving frequency for Graphite/Epoxy laminated simply supported beam for  $[0^\circ/75^\circ]_s$  at temperatures 22, 40, and  $60^\circ\text{C}$

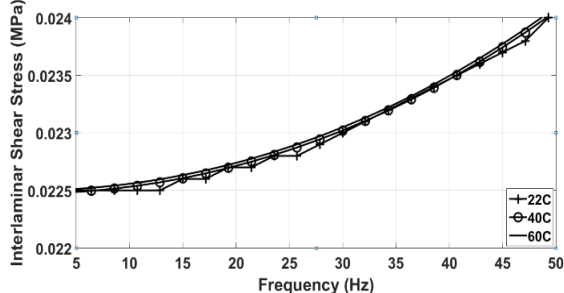


**Figure 18.** Relation between mid-plane interfacial shear stress and driving frequency for Graphite/Epoxy laminated simply supported beam for  $[0^\circ/90^\circ]_s$  at temperatures 22, 40, and  $60^\circ\text{C}$

Comparing mid-plane harmonic deflection and shear stress of simply supported composite beam considered for all fiber orientations ( $[0^\circ]_s$ ,  $[0^\circ/15^\circ]_s$ ,  $[0^\circ/30^\circ]_s$ ,  $[0^\circ/45^\circ]_s$ ,  $[0^\circ/60^\circ]_s$ ,  $[0^\circ/75^\circ]_s$ , and  $[0^\circ/90^\circ]_s$ ) across frequency range 5 - 50Hz Hz at temperatures 22, 40, and  $60^\circ\text{C}$  shows that highest and lowest deflections are recorded for schemes  $[0/60]_s$  and  $[0^\circ]_s$  respectively. This is reasonable since the latter scheme leads to a structure with much higher strength than all other fiber orientation schemes. It is also noted that schemes  $[0^\circ/60^\circ]_s$ ,  $[0^\circ/90^\circ]_s$ , and  $[0^\circ/45^\circ]_s$  undergo much higher transverse deflections than other schemes. Furthermore, it should be observed that maximum shear stress existing between layers at midplane undergoes close range values for most of the schemes except at the orientation scheme  $[0^\circ]_s$  where large values are recorded due to large strength of this orientation scheme.

### 5. Limitation and Future scope

Accuracy of finite element results remain an issue when solving for stresses when sudden change in geometry occurs. As a result, induced stresses may be larger at these locations than the yield stress since linear finite element analysis may not predict results accurately. However, studying dynamic facial shear stresses in laminated FRP

spherical and cylindrical shells is highly recommended to investigate the failure of such structures with different boundary conditions due to temperature and frequency effect using FE analysis.

### 6. Conclusion

This work investigates dynamic behavior of Graphite/Epoxy FRP eight-layer laminated simply supported beam at different temperatures (22, 40, and  $60^\circ\text{C}$ ) and for fiber orientation schemes ( $[0]_s$ ,  $[0^\circ/15^\circ]_s$ ,  $[0^\circ/30^\circ]_s$ ,  $[0^\circ/45^\circ]_s$ ,  $[0^\circ/60^\circ]_s$ ,  $[0^\circ/75^\circ]_s$ , and  $[0^\circ/90^\circ]_s$ ) across frequency variation 5-50 Hz using finite element package ANSYS19.

Modal analysis is carried out to find out the first six natural frequencies for all fiber orientation schemes and temperatures considered where results showed that natural frequencies drop slightly for all the schemes considered at each temperature.

It is found that higher natural frequencies are obtained for fiber orientation scheme  $[0]_s$  where highest natural frequencies are recorded at fiber orientation scheme  $[0^\circ]_s$  as 258.56, 258.4, and 258.23 Hz at temperatures 22, 40 and  $60^\circ\text{C}$  respectively.

Concerning the harmonic analyses, it should be mentioned that both interfacial mid-plane transverse deflection and shear stress responses are found to increase narrowly when increasing temperature for all schemes considered. Moreover, it is concluded that  $[0]_s$  case presents a significant scheme since it undergoes minimum transverse deflection and maximum shear stress at each single temperature compared with other schemes. Also, it should be noted that specific shear stress responses share almost the same results at temperatures 40 and  $60^\circ\text{C}$  as results show in  $[0^\circ/30^\circ]_s$ ,  $[0^\circ/45^\circ]_s$  cases.

Largest transverse deflection recorded is 82.7mm at frequency 285Hz and temperature  $22^\circ\text{C}$  when modeling the simply supported beam for with  $[0]_s$  orientation scheme. However, maximum shear stress value 81.2 MPa is obtained at the same fiber orientation for temperature  $60^\circ\text{C}$

### Acknowledgements

This work was supported by Al-Balqa Applied University. In addition, Ali Al-Foqaha presented a helpful data throughout this study.

### References

- [1] Li, F., Deng, A. Z., Zhao, Q. L., & Duan, J. (2020). Research on Influence mechanism of composite interlaminar shear strength under normal stress. *Science and Engineering of Composite Materials*, 27(1), 119–128. <https://doi.org/10.1515/secm-2020-0011>
- [2] Tabiei, A., & Zhang, W. (2018). Composite laminate delamination simulation and experiment: A review of recent development. In *Applied Mechanics Reviews* (Vol. 70, Issue 3). American Society of Mechanical Engineers (ASME). <https://doi.org/10.1115/1.4040448>
- [3] Roudsari, S., Hamoush, S., Soleimani, S., Abu-Lebdeh, T., & Haghhighifar, M. (2018). Analytical Study of Reinforced Concrete Beams Strengthened by FRP Bars Subjected to Impact Loading Conditions. *American Journal of Engineering and Applied Sciences Original Research Paper*. <https://doi.org/10.3844/ajeassp.2018>
- [4] Alsaadi, M., Uglu, A. A., & Erklig, A. (2017). A comparative study on the interlaminar shear strength of carbon, glass, and Kevlar fabric/epoxy laminates filled with SiC particles.

- Journal of Composite Materials*, 51(20), 2835–2844. <https://doi.org/10.1177/0021998317701559>
- [5] Eskandari, S., Andrade Pires, F. M., Camanho, P. P., Cui, H., Petrinic, N., & Marques, A. T. (2019). Analyzing the failure and damage of FRP composite laminates under high strain rates considering visco-plasticity. *Engineering Failure Analysis*, 101, 257–273. <https://doi.org/10.1016/j.engfailanal.2019.03.008>
- [6] Chandra Ray, B., & Rathore, D. (2015). A review on mechanical behavior of FRP composites at different loading speeds. In *Critical Reviews in Solid State and Materials Sciences* (Vol. 40, Issue 2, pp. 119–135). Taylor and Francis Inc. <https://doi.org/10.1080/10408436.2014.940443>
- [7] Rakesh, P. K., Sharma, V., Singh, I., & Kumar, D. (2011). *Delamination in Fiber Reinforced Plastics: A Finite Element Approach*, 3, 549–554. <https://doi.org/10.4236/eng.2011.34064>
- [8] Chakraborty, D. (2007). Delamination of laminated fiber reinforced plastic composites under multiple cylindrical impact. *Materials and Design*, 28(4), 1142–1153. <https://doi.org/10.1016/j.matdes.2006.01.029>
- [9] Elmalich, D., & Rabinovitch, O. (2015). Dynamic Geometrically Nonlinear Behavior of FRP-Strengthened Walls with Debonded Regions. *Journal of Engineering Mechanics*, 141(1), 04014105. [https://doi.org/10.1061/\(asce\)em.1943-7889.0000814](https://doi.org/10.1061/(asce)em.1943-7889.0000814)
- [10] Sankara Babu Ch. S., Rao, V. T., & Kumar, S. B. (2018). *Effect of Fiber Angle on Interlaminar Stresses of FRP Angle Ply Laminate* (Vol. 6, Issue 1). [www.ijcrt.org](http://www.ijcrt.org)
- [11] Imran, M., Khan, R., & Badshah, S. (2019). Investigating the effect of delamination size, stacking sequences and boundary conditions on the vibration properties of carbon fiber reinforced polymer composite. *Materials Research*, 22(2). <https://doi.org/10.1590/1980-5373-MR-2018-0478>
- [12] Islam, M. S., & Prabhakar, P. (2017). Modeling framework for free edge effects in laminates under thermo-mechanical loading. *Composites Part B: Engineering*, 116, 89–98. <https://doi.org/10.1016/j.compositesb.2017.01.072>
- [13] Li, J., Fan, W., Liu, T., Yuan, L., Xue, L., Dang, W., & Meng, J. (2020). The temperature effect on the inter-laminar shear properties and failure mechanism of 3D orthogonal woven composites. In *Textile Research Journal* (Vol. 90, Issues 23–24, pp. 2806–2817). SAGE Publications Ltd. <https://doi.org/10.1177/0040517520927009>
- [14] Liu, Z., Yang, Z., Chen, Y., Yu, Y., Wei, Y., Li, M., & Huang, C. (2020). Dynamic tensile and failure behavior of bi-directional reinforced GFRP materials. *Acta Mechanica Sinica/Lixue Xuebao*, 36(2), 460–471. <https://doi.org/10.1007/s10409-019-00920-8>
- [15] Mahato, K. K., Dutta, K., & Ray, B. C. (2018). Static and Dynamic Behavior of Fibrous Polymeric Composite Materials at Different Environmental Conditions. *Journal of Polymers and the Environment*, 26(3), 1024–1050. <https://doi.org/10.1007/s10924-017-1001-x>
- [16] Panda, S. K., & Pradhan, B. (2007). Thermoelastic analysis of the asymmetries of interfacial embedded delamination characteristics in laminated FRP composites. *Composites Part A: Applied Science and Manufacturing*, 38(2), 337–347. <https://doi.org/10.1016/j.compositesa.2006.03.012>
- [17] Shivakumar, K., Pora, A., & Abali, F. (n.d.). INTERLAMINAR SHEAR TEST FOR LAMINATED TEXTILE FABRIC COMPOSITES.
- [18] Das, R. R., Singla, A., & Srivastava, S. (2016). Thermo-mechanical Interlaminar Stress and Dynamic Stability Analysis of Composite Spherical Shells. *Procedia Engineering*, 144, 1060–1066. <https://doi.org/10.1016/j.proeng.2016.05.058>
- [19] Wang, X., Zhao, X., Wu, Z., Zhu, Z., & Wang, Z. (2016). Interlaminar shear behavior of basalt FRP and hybrid FRP laminates. *Journal of Composite Materials*, 50(8), 1073–1084. <https://doi.org/10.1177/0021998315587132>
- [20] Al-Huniti, N., Al-Faqs, F., & Abu Zaid, O. (2010). Finite Element Dynamic Analysis of Laminated Viscoelastic Structures. *Applied Composite Materials*, 17(4), 405–414. <https://doi.org/10.1007/s10443-010-9129-z>
- [21] Alfaqs, F. (2020). Dynamic analysis of thin laminated viscoelastic structures under elevated temperature using finite element modeling. *Naukovyi Visnyk Natsionalnoho Hirnychoho Universytetu*, 2020(6), pp. 28-33. <https://doi.org/10.33271/mvngu/2020-6/028>
- [22] Alfaqs, F., Haddad, J., Fayyad, S., Koroviaka, Y., Rastsvietaiev, V., Effect of Elevated Temperature on Harmonic Interlaminar Shear Stress in Graphite/Epoxy FRP Simply Supported Laminated Thin Plate Using Finite Element Modeling, (2020) International Review of Mechanical Engineering (IREME), 14 (8), pp. 523-533. <https://doi.org/10.15866/ireme.v14i8.1946>
- [23] Imran, M., Khan, R., Badshah, S. (2021). 'Experimental, analytical, and finite element vibration analyses of delaminated composite plates', *Scientia Iranica*, 28(1), pp. 231-240. doi: 10.24200/sci.2019.51508.2223
- [24] Imran, M., Badshah, S., & Khan, R. (2019). Vibration Analysis of Cracked Composite Laminated Plate: A Review. *Mehran University Research Journal Of Engineering And Technology*, 38(3), 705-716. doi:10.22581/muet1982.1903.14
- [25] Ghadiri, M., Malekzadeh, K., & Ghasemi, F. A. (2015). Free Vibration of an Axially Preloaded Laminated Composite Beam Carrying a Spring-Mass-Damper System with a NonIdeal Support. *Jordan Journal of Mechanical & Industrial Engineering*, 9(3), pp. 195-207
- [26] Gharaibeh, M., Ismail, Adel A., Al-Shammery, Ahmad F., Ali, Omar A. (2019). Three-Material Beam: Experimental Setup and Theoretical Calculations. *Jordan Journal of Mechanical & Industrial Engineering*, 13(4) pp. 253-264.
- [27] [21] Gu, H., Chattopadhyay, A., Li, J., & Zhou, X. (2000). A higher order temperature theory for coupled thermo-piezoelectric-mechanical modeling of smart composites. *International Journal of Solids and Structures*, 37(44), pp.6479–6497. [https://doi.org/10.1016/s0020-7683\(99\)00283-8](https://doi.org/10.1016/s0020-7683(99)00283-8)
- [28] [22] Tahani, M., & Nosier, A. (2003). Free edge stress analysis of general cross-ply composite laminates under extension and thermal loading. *Composite Structures*, 60(1), pp.91–103. [https://doi.org/10.1016/s0263-8223\(02\)00290-8](https://doi.org/10.1016/s0263-8223(02)00290-8).